

Structures of Liquid Crystalline Wholly Aromatic Copolyester Films with Different Copolymer Compositions

KOICHIRO YONETAKE,* MITSURU SHINOHARA, and TORU MASUKO

Faculty of Engineering, Yamagata University, Jonan 4, Yonezawa, Yamagata, 992 Japan

SYNOPSIS

Films of wholly aromatic copolyester composed of 4-hydroxybenzoic acid (HBA) and 2-hydroxy-6-naphthoic acid (HNA) were prepared by a solution-casting method using a mixed solution of pentafluorophenol (PFP) and chloroform (weight ratio: PFP/chloroform = 3/7). Using five samples with different copolymer compositions (HBA/HNA [mol %] = 25/75, 40/60, 55/45, 62/38, 73/27), the effects of the copolymer composition on the fine structures of the films were investigated using thermal analyses, density measurements, X-ray diffraction methods, and tensile tests. The as-cast films obtained were shown to be transparent and highly amorphous in spite of changing the copolymer composition. When the films were heated above the T_g (100°C), cold crystallization first occurred during the heating process and they had melting points. The densities of the films increased with increasing annealing temperature throughout the cold crystallization. The elongation percentages of the as-cast films reached high values of 30–74% at room temperature, indicating their maximum of elongation at 55 mol % of HBA. © 1996 John Wiley & Sons, Inc.

INTRODUCTION

The wholly aromatic copolyester composed of 4-hydroxybenzoic acid (HBA) and 2-hydroxy-6-naphthoic acid (HNA) (HBA/HNA copolymer) exhibits complicated fine structures in their solid states, since they are formed by the extended chains with random comonomeric sequences.^{1,2} Several models of crystallization in such types of copolyesters have been proposed in terms of the complicatedly coagulated structures.^{3–6} The morphology of the copolymer is strongly dependent on its thermal history.^{5,7} The crystal growth occurs on annealing above the glass transition temperature, and the packing mode of the molecular chains in the crystallite changes on annealing.^{5,7–9} In conjunction with the above results, phase transitions,^{7,10} chain mobility,^{11,12} and physical properties^{13,14} of HBA/HNA copolymers have been investigated using injection-molded or melt-spun fiber samples prepared from their anisotropic nematic melt.

Windle et al.^{15,16} examined the morphology of the copolymer using highly sheared thin films, having found two kinds of fine structures (banded and tight textures) which were characteristic of extended chains. Formation of these textures depended on the shearing speed during the film preparation.

Generally, a highly oriented structure is formed in copolymer films prepared from the nematic melt by an extruded molding method. The film prepared in this way is opaque and indicates anisotropic mechanical properties: The strength normal to the machine direction (MD) is extremely lower than that parallel to MD. It is necessary to improve such optical and mechanical properties.

We prepared the highly amorphous and transparent thin film of the copolymer (HBA/HNA = 73/27) by the solution-casting method and examined the phase transition of the copolymer film during the annealing process.¹⁷ The glass transition, cold crystallization, and nematic texture were clearly observed using the solution-cast film.¹⁷ In this article, we investigated the effects of the copolymer compositions of HBA/HNA copolymers on the fine structures of the solution-cast films using X-ray diffraction and thermal analyses.

* To whom correspondence should be addressed.

EXPERIMENTAL

Materials and Film Preparation

Five HBA/HNA copolyesters with different copolymer compositions were used: HBA/HNA (mol %) = 25/75, 40/60, 55/45, 62/38, and 73/27. They were synthesized by Calundann's method.¹⁸ The intrinsic viscosities of them were 6.6–7.5 dL g⁻¹ in a mixed solution of pentafluorophenol (PFP)/chloroform.

The films were prepared using a solution-casting method with the mixed solution. The weight ratio of the mixed solution (PFP/chloroform) was 3/7. The film preparation method was described in our previous article.¹⁷ The thickness of each film was about 20 μm. These films are coded as C-25, C-40, C-55, C-62, and C-73, where the numbers denote the volume fraction of HBA.

Polarizing Optical Microscopy and Scanning Electron Microscopy

The HBA/HNA copolymer films were examined during a heating process using a polarizing optical microscope equipped with a hot stage (Linkam Co., TH-600RMS). The heating rate was programmed as 30°C min⁻¹. The fracture surfaces of above solution-casting films which were broken in liquid nitrogen were observed at 25 kV under a scanning electron microscope JSM-5300 (JEOL Ltd.).

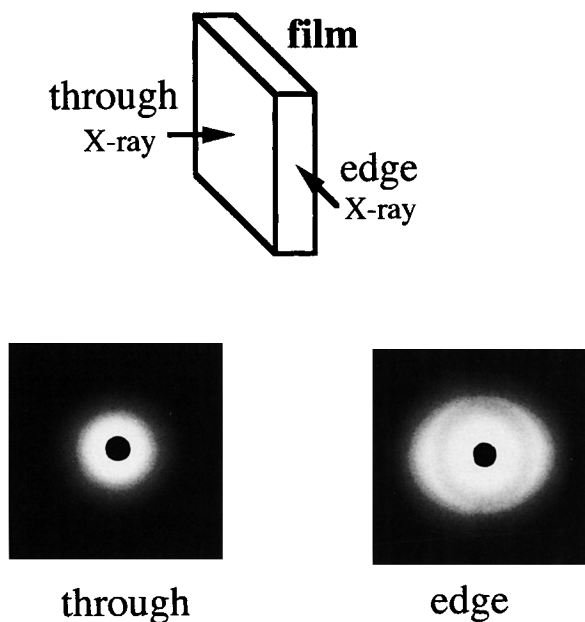


Figure 1 WAXS patterns of through and edge views for the as-cast film of C-73.

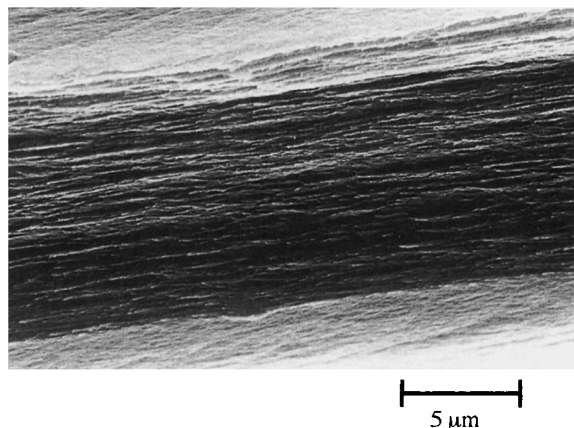


Figure 2 Scanning electron micrograph for the fractured surface of the as-cast film of C-73.

Thermal Properties

The thermal properties of the films were investigated using a differential scanning calorimeter (DSC 200; Seiko Instruments & Electronics Ltd.) under a N₂ purge; heating and cooling rates were 30 and 20°C min⁻¹, respectively.

Density Measurement

Densities (ρ) of the films were measured at 30°C using a density gradient column filled with an aqueous solution of calcium bromide.

X-ray Diffraction Measurements

X-ray diffraction experiments were carried out by a RAD-rA diffractometer (Rigaku Denki Co. Ltd.) equipped with a heating device. Nickel-filtered CuK α radiation was employed. Changes in the wide-angle X-ray scattering (WAXS) traces during stepwise heating and cooling processes were recorded by a scintillation counter system with a 1.0 mm-diameter pinhole collimator and 1 × 1° receiving slit. The diffractometry was performed in transmission. The temperature accuracy of the heating device used was $\pm 0.2^\circ\text{C}$. WAXS traces were obtained by a step-scanning method: The step width and fixed time were programmed for steps of 0.05° every 4 s. When d -spacings of the reflections were measured, the step and fixed time were programmed for an angle of 0.01° and a 10 s step, respectively. The accuracy of the d -value measurements was better than $\pm 5 \times 10^{-4}$ nm. The WAXS photographs were taken by a flat Laue camera with a 0.5 mm-diameter pinhole collimator.

Mechanical Properties

Tensile measurements for the sample films were carried out using an Autograph DCS-50M (Shimadzu Ltd.) at room temperature. The width of the films was 1 mm. The distance between the machine chucks and the strain rate were programmed at 20 mm and 10 mm/min, respectively. The tensile strength, tensile moduli, and elongations of the films were measured.

RESULTS AND DISCUSSION

Morphology of Solution-casting Films with Various Copolymer Compositions

The solution-cast films obtained were transparent and colorless, and they exhibited a dark field under crossed polarizers in spite of various copolymer compositions. Melt-cast films prepared from the nematic melt (melt-pressed samples) appeared milk white and opaque in comparison with the above solution-cast films with similar thickness. In addition, only a diffuse halo was observed in the WAXS pattern of each solution-cast film. Consequently, they were highly amorphous and they might have very small glassy nematic domains. The morphology of the films was probably formed through an isotropic gel state at the comparatively low temperature (27°C) in the solution-casting procedure.

Figure 1 shows the WAXS patterns of through and edge views for the solution-cast film of C-73. The WAXS pattern of the through view indicated

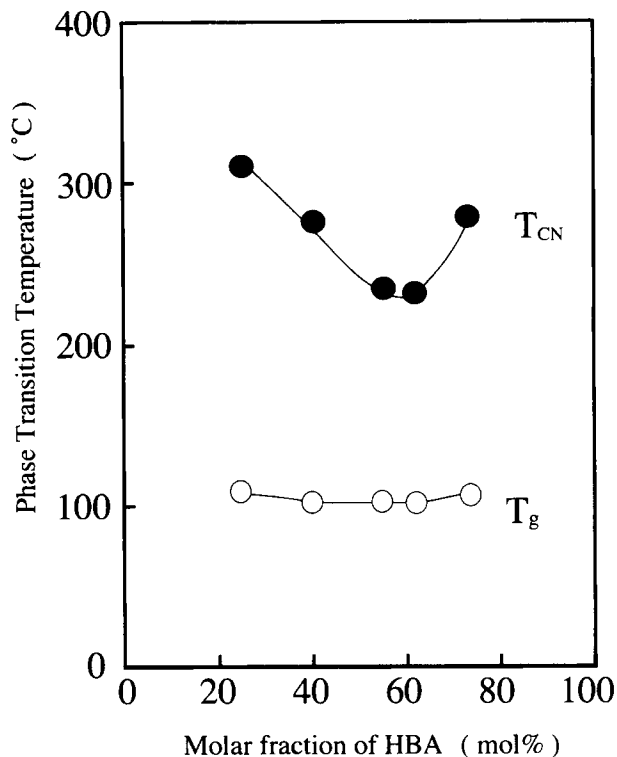


Figure 4 Changes in phase transition temperatures (T_{CN} and T_g) of the as-cast films with the molar fraction of HBA.

a diffuse halo, while a diffuse arc was observed in the edge-view pattern. The scanning electron micrograph for the edge view of the as-cast film C-73 is shown in Figure 2, where a layer structure is clearly observed. The layers exist parallel to the film

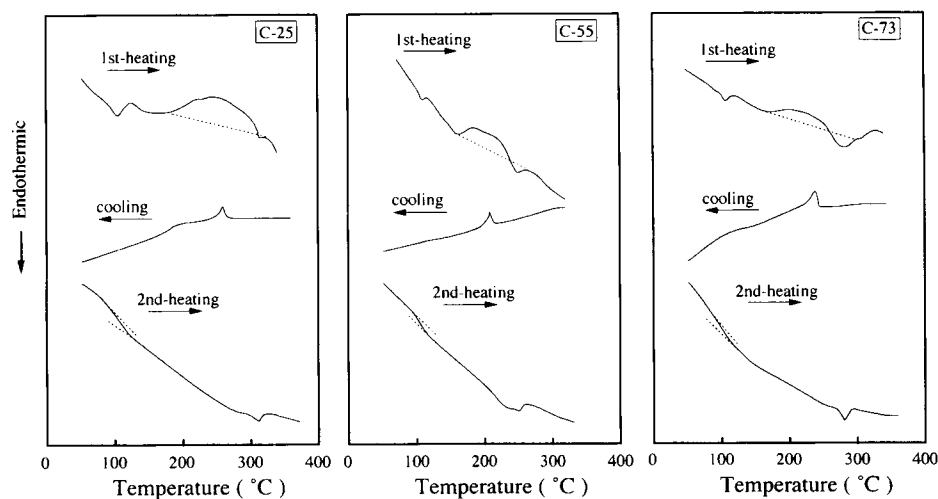


Figure 3 DSC traces of as-cast films for C-25, C-55, and C-73 during heating and cooling processes.

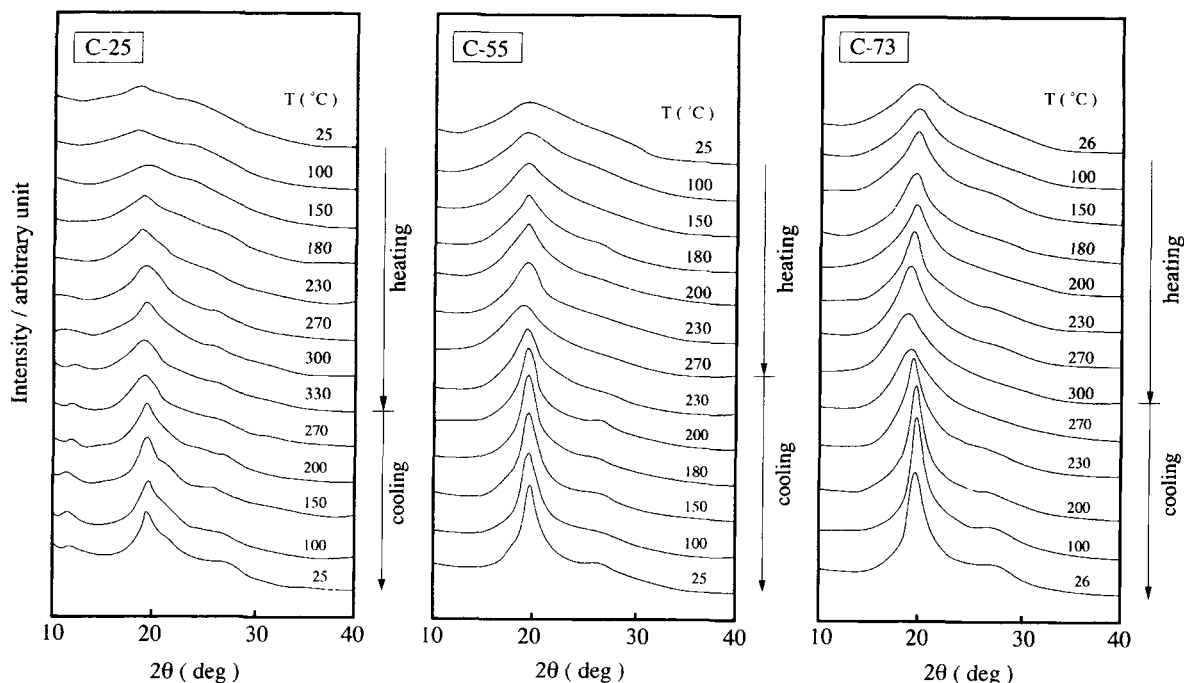


Figure 5 WAXS curves of as-cast films for C-25, C-55, and C-73 during heating and cooling processes.

plane. These indicate a very low level of uniplanar orientation. Other films showed similar WAXS patterns in the edge views characteristic of the layer structures. Such a morphology of the solution-cast films is something different from a completely amorphous state of ordinary flexible polymers.

Effects of the Copolymer Compositions on the Structural Changes of the As-cast Films

The as-cast film of C-73 clearly indicated the glass transition (T_g) at 110°C, a broad exothermic peak at 150°C, and an endothermic peak corresponding to the crystal/nematic transition (T_{CN}) at 280°C on the first heating process.¹⁷ Figure 3 compares DSC traces of the as-cast films for C-25, C-55, and C-73. The DSC traces of C-25 and C-55 films are similar to that of C-73. With the second heating process, a base-line shift at the T_g 's and an endothermic peak corresponding to T_{CN} are observed with no exothermic peak. The second heating traces were similar to those of the melt-pressed or molded samples,^{10,19} since the films were heated up to the nematic melt state. The films were opaque after the above annealing treatment. After the second heating process, the thermal behaviors of the samples were reversible. Similar thermal behaviors were observed

in other as-cast films: They also showed exothermic peaks above the T_g 's with the first heating process.

For examination of composition dependence, the T_g 's and T_{CN} 's of these films obtained by DSC measurements are plotted with the molar fraction of HBA in Figure 4. The T_g 's remain almost unchanged in spite of varied copolymer compositions. The T_{CN} 's indicate the minimum value at 55 mol % of HBA. The composition dependence on the T_{CN} 's coincides with the melt-pressed samples, which is ascribed to the random comonomeric sequences of HBA and HNA.²⁰

Figure 5 shows WAXS traces at elevated temperatures for the as-cast films of C-25, C-55, and C-73 during the heating and cooling processes. As described earlier, the WAXS traces obtained at room temperature (25°C) show that the samples remain highly amorphous. The Bragg's reflections ($2\theta = 19^\circ\text{--}27^\circ$) appear in the traces above 150°C and their intensities increase gradually on heating up to their T_{CN} 's. The temperature range from 150°C to T_{CN} corresponds to the exothermic peak range in the DSC curve of each film. In relation to this, the light intensity of birefringence increased with increasing temperature above 150°C under the polarizing optical microscope. As described in the previous article,¹⁷ the packing mode of the copolymer

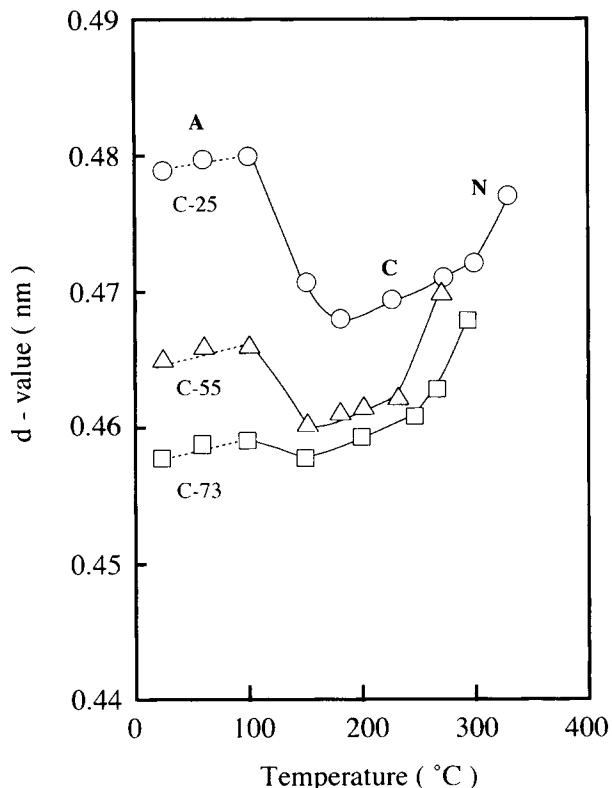


Figure 6 Changes in d values of the amorphous scattering peaks and 110 reflections of the orthorhombic crystal for the as-cast films of (○) C-25, (△) C-55, and (□) C-73 with temperature during the heating process. The dotted line denotes the d value of the amorphous peak and the solid line that of the 110 reflection. A: Amorphous state; C: crystal state, N: nematic state.

chains were forced to change and the crystalline-ordered structures formed in the temperature range.

When the samples were cooled from the nematic melt, the WAXS curves become comparatively sharp as shown in Figure 5. This implies that the crystallinity of the samples increases after annealing effects. Similar fine structural changes were observed in other films with different copolymer compositions.

Figure 6 illustrates changes in the d values of the WAXS intensity maxima of the as-cast films (C-25, C-55, and C-73) against temperature with their first heating processes. Since these solution-cast films are highly amorphous, the d values measured below T_g correspond mostly to those of the amorphous scattering peaks. They were measured at their maximum intensities. The films might have small glassy nematic domains, but it was impossible to distinguish the amorphous and glassy nematic scattering peaks on the WAXS patterns. The d values measured in

above temperature range are shown by broken lines in Figure 6. They increase linearly with the thermal expansion of the glassy state on heating up to T_g and then decrease suddenly above the T_g . The sharp WAXS patterns characteristic of some Bragg's reflections appeared in the higher temperature range where the d values continue to decrease. This comes from the fact that the more ordered chain coagulation occurs as the chain mobility is enhanced by heating above the T_g .

After reaching the minimum, the d values increase with increasing temperature again. In the case of C-73, the d value agrees with that of the 110 reflection for the orthorhombic crystal of the highly oriented fiber sample containing 73 mol % of HBA.^{19,21} The d values for C-25 and C-55 obtained above 200 and 180°C, respectively, are consistent with those of 110 reflections measured from the fiber samples.^{19,21} Consequently, cold crystallization by the molecular chain rearrangement occurs in the film, since molecular chain mobility is enhanced at a high temperature above the T_g .

The d values increase more with increasing temperature on further heating above its T_{CN} as shown in Figure 6. The linear expansion coefficients estimated from the slopes represents the value of the

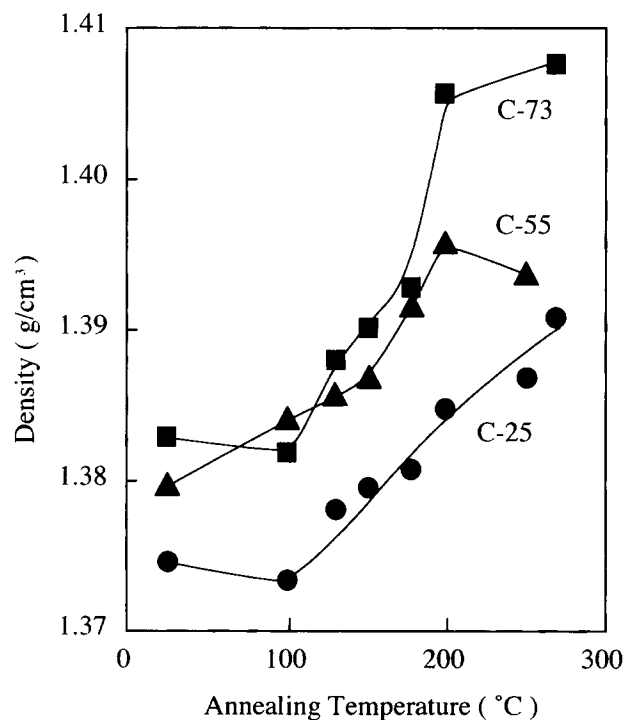


Figure 7 Changes in density of films with annealing temperature. The films were annealed at various annealing temperatures for 1 h: (●) C-25; (▲) C-55; (■) C-73.

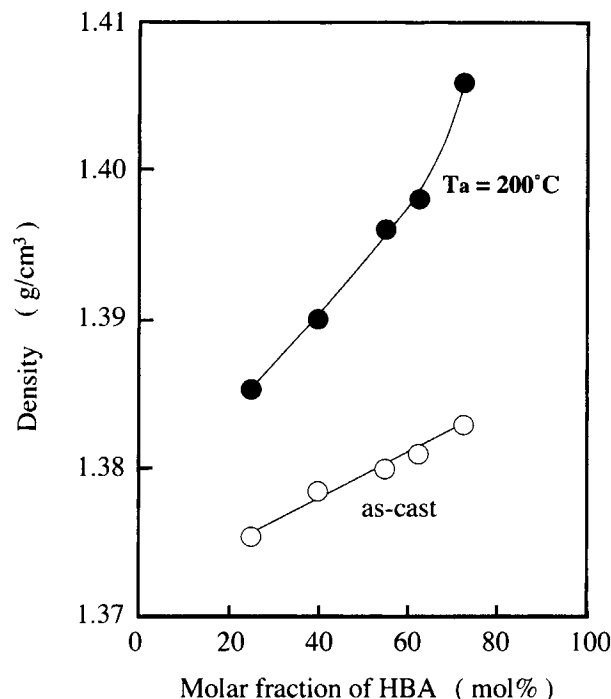


Figure 8 Changes in density of the films with molar fraction of HBA; the as-cast films and the films were annealed at 200°C for 1 h.

10^{-4} order, which is associated with the mesomorphic state.

Annealing Effects on the Films with Various Copolymer Compositions

The solution-cast films were annealed at various annealing temperatures for 1 h using the DSC device in a N_2 purge. Figure 7 shows the densities of annealed C-25, C-55, and C-73 films plotted against the annealing temperature. The density of each film annealed below the T_g corresponds to that of the amorphous copolymer. The densities increase above the T_g which is accompanied by the cold crystallization described in the preceding section. No remarkable change in density of the melt-pressed samples was observed in the above temperature range. The melt-pressed samples or melt-spun fibers have a comparatively higher denser state, even if the samples were quenched, because the amorphous state cannot be frozen in these ordinarily quenched samples from the melt. Consequently, the density can be changed widely by the annealing treatment in the case of the solution-cast films.

Figure 8 shows changes in the densities of the films with the molar fraction of HBA. The open

symbol denotes the densities of the as-cast films, and the closed symbol, those of films annealed at 200°C for 1 h. The densities of the as-cast films increase with an increasing HBA molar fraction. There is a linear relationship between the density and molar fraction of HBA. The specific volume of the HBA chain is smaller than that of the HNA chain, since the HBA chain is more linear as compared with the HNA chain. Thus, the HBA-rich film is denser than is the HNA-rich film.

The densities of the annealed films also increase with the HBA molar fraction. Particularly, those of the HBA-rich films exhibit very high values. In general, the density of an annealed sample is due to the crystallinity, as well as being dependent on the crystal density itself. The crystal densities of PHBA and PHNA were estimated to 1.49 and 1.45 g/cm^3 , respectively, using their lattice parameters.^{5,22} As a result, the densities of the annealed HBA-rich films become higher than those of the annealed HNA-rich ones.

Mechanical Properties of the Films

The solution-cast films exhibited isotropic mechanical properties in the tensile test. Figure 9 shows the stress-strain curves of the films measured at room temperature. The elongations of the as-cast films are very high as compared with those of the melt-pressed samples. The high elongation of the solution-cast films probably results from their highly amorphous structures. Generally, the elongation of the melt-pressed samples or melt-spun fibers is only several percent because they have higher crystallin-

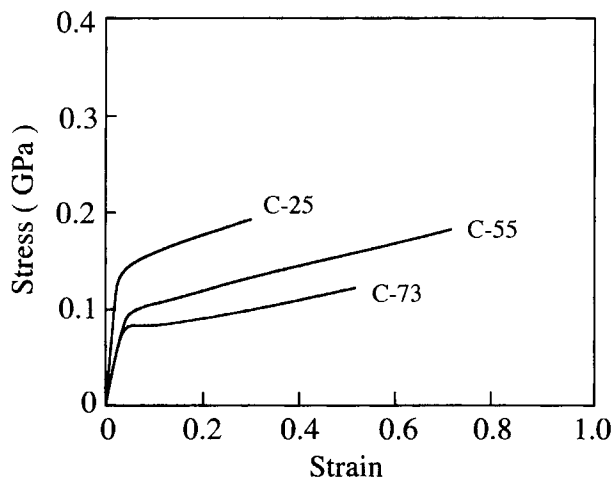


Figure 9 Stress-strain curves of as-cast films for C-25, C-55, and C-73.

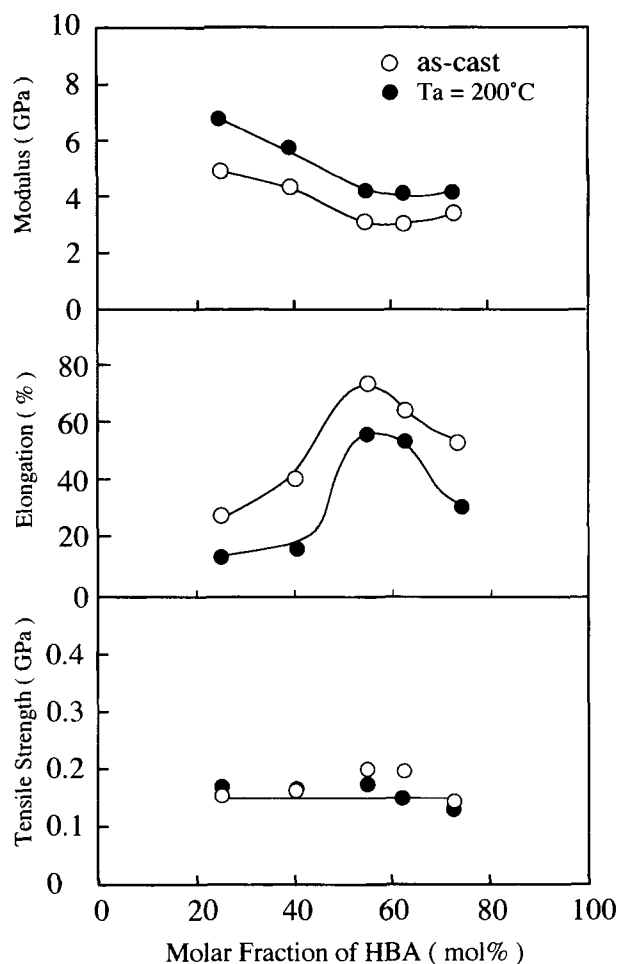


Figure 10 Changes in tensile modulus, elongation, and strength of the as-cast films with the molar fraction of HBA.

ity; additionally, the fibers are already highly oriented in the spinning process.^{23,24}

As shown in Figure 10, the tensile strength of the as-cast films is not so high, even if they are annealed. It implies that the tensile strength of the liquid crystalline polymers depends preferentially on the orientation of molecular chains.

Changes in strength, elongation, and modulus against the molar fraction of HBA are shown in Figure 10. There is the maximum of elongation at 55 mol % of HBA. The highest elongation, 74%, of C-55 presumably comes from the low crystallinity, i.e., the orientational crystallization does not occur easily during the stretching process because of its random sequence of the copolymer chain. The strength and modulus do not indicate a strong dependency on the copolymer composition. At this time, we cannot explain the origin of above me-

chanical properties in terms of these limited results. Morphological changes and the orientational mechanism of the films are now being studied in our laboratory and will be reported in the near future.

CONCLUSION

1. The solution-cast films were transparent and highly amorphous in spite of the varied copolymer compositions.
2. In each film, cold crystallization occurred during the heating process by the molecular chain rearrangement, since molecular chain mobility was enhanced above the T_g .
3. The densities increased with increasing annealing temperature throughout the cold crystallization. The density of the HBA/HNA copolymers can be changed drastically using the solution-cast film.
4. The elongation percentages of the as-cast films showed very high values of 30–74% at room temperature. There was a maximum of elongation at 55 mol % of HBA.

REFERENCES

1. G. A. Gutierrez, R. A. Chivers, J. Blackwell, J. B. Stamatoff, and H. Yoon, *Polymer*, **24**, 937 (1983).
2. J. Blackwell, G. A. Gutierrez, and R. A. Chivers, *Macromolecules*, **17**, 1219 (1984).
3. D. J. Blundell, *Polymer*, **23**, 359 (1982).
4. A. H. Windle, C. Viney, R. Golombok, A. M. Donald, and G. R. Mitchell, *Faraday Discuss. Chem. Soc.*, **79**, 55 (1985).
5. X.-C. Fa and T. Takahashi, *Sen-i Gakkaishi*, **46**, 49 (1990).
6. S. D. Hudson and A. J. Lovinger, *Polymer*, **34**, 1123 (1993).
7. A. Kaito, M. Kyotani, and K. Nakayama, *Macromolecules*, **23**, 1035 (1990).
8. A. Flores, F. Ania, F. J. B. Calleja, and I. M. Word, *Polymer*, **34**, 2915 (1993).
9. D. J. Wilson, C. G. Vonk, and A. H. Windle, *Polymer*, **34**, 227 (1993).
10. M.-Y. Cao and B. Wunderlich, *J. Polym. Sci. Polym. Phys. Ed.*, **23**, 521 (1985).
11. J. Clements and J. Humphreys, *J. Polym. Sci. Polym. Phys. Ed.*, **24**, 2293 (1986).
12. G. R. Mitchell and F. Ishii, *Polym. Commun.*, **26**, 34 (1985).

13. D. J. Blundell and K. A. Buckingham, *Polymer*, **26**, 1623 (1985).
14. M. J. Troughton, A. P. Unwin, G. R. Davies, and I. M. Ward, *Polymer*, **29**, 1389 (1988).
15. R. J. Spontak and A. H. Windle, *Polymer*, **31**, 1395 (1990).
16. S. E. Bedford and A. H. Windle, *Polymer*, **31**, 616 (1990).
17. K. Yonetake, T. Sagiya, K. Koyama, and T. Masuko, *Macromolecules*, **25**, 1009 (1992).
18. G. W. Calundann, U.S. Pat. 4,161,470 (1979).
19. K. Yonetake, N. Kamba, K. Sasaki, K. Koyama, and T. Masuko, *Rep. Progr. Polym. Phys. Jpn.*, **33**, 199 (1990).
20. G. W. Calundann and M. Jaffe, *Proc. Robert A Welch Found. Conf. Chem. Res.*, **26**, 246 (1983).
21. N. Kamba, K. Yonetake, K. Koyama, K. Sasaki, and T. Masuko, *Polym. Prepr. Jpn.*, **39**, 751 (1990).
22. Y. Yamashita, K. Monobe, Y. Kato, S. Endo, and K. Kimura, *Polym. Prepr. Jpn.*, **35**, 876 (1986).
23. D.-K. Yang and W. R. Krigbaum, *J. Polym. Sci. Polym. Phys. Ed.*, **27**, 1837 (1989).
24. J. Sarlin and P. Tormala, *J. Appl. Polym. Sci.*, **40**, 453 (1990).

Received February 13, 1996

Accepted May 15, 1996